

**Coronal activity from the ASAS eclipsing binaries**

by

Szczygiel<sup>1</sup>, D. M., Socrates<sup>2</sup>, A., Paczyński<sup>2</sup>, B., Pojmański<sup>1</sup>, G.,  
Pilecki<sup>1</sup>, B.<sup>1</sup>Warsaw University Observatory, Al. Ujazdowskie 4, 00-478 Warsaw, Poland  
e-mail: dszczyg, gp, pilecki@astrouw.edu.pl<sup>2</sup>Princeton University Observatory, Peyton Hall, Princeton, NJ 08544, USA  
e-mail: socrates@astro.princeton.edu*Received Month Day, Year*

## ABSTRACT

We combine the catalogue of eclipsing binaries from the *All Sky Automated Survey (ASAS)* with the *ROSAT All Sky Survey (RASS)*. The combination results in 836 eclipsing binaries that display coronal activity and is the largest sample of active binary stars assembled to date. By using the (*V-I*) colors of the ASAS eclipsing binary catalogue, we are able to determine the distances and thus bolometric luminosities for the majority of eclipsing binaries that display significant stellar activity. A typical value for the ratio of soft X-ray to bolometric luminosity is  $L_X/L_{\text{bol}} \sim \text{a few} \times 10^{-4}$ , similar to the ratio of soft X-ray to bolometric flux  $F_X/F_{\text{bol}}$  in the most active regions of the Sun. Unlike rapidly rotating isolated late-type dwarfs – stars with significant outer convection zones – a tight correlation between Rossby number and activity of eclipsing binaries is absent. We find evidence for the saturation effect and marginal evidence for the so-called “super-saturation” phenomena. Our work shows that wide-field stellar variability searches can produce a high yield of binary stars with strong coronal activity.

The combined ASAS and RASS catalogue, as well as the results of this work are available for download in a form of a file.

**Key words:**

stars: eclipsing – stars: binary – stars: evolution – stars: X-rays

**1. Introduction**

In the last few decades, it has become clear that chromospheric and coronal activity of main sequence dwarfs is intimately tied to stellar rotation rate. Main sequence stars are born rapidly rotating and quickly lose their angular momentum by some combination of stellar winds and magnetic torques. It follows that stars with rapid rotation – ideal for studies of stellar activity – are quite rare.

In comparison to isolated main sequence stars, close eclipsing binaries are rare as well. However, they are dramatically variable in comparison to rapidly rotating single stars. Close binaries that consist of two late-type dwarfs are thought to be synchronized as long as their orbital periods are shorter than 10 days or so (Duquennoy & Mayor, 1991). This is true for the majority of close binaries, which then may be fruitfully employed in a study of stellar activity.

Contact binary stars were discovered to be strong X-ray emitters almost 30 years ago (Carroll et al. 1980). Shortly afterward Cruddace and Dupree (1984) identified 14 X-ray active W UMa systems and noticed a correlation between X-ray luminosity and rotational period, suggesting that for very fast rotators this relation may be reversed. Since then, the study of W UMa activity has broadened – X-ray flux variations were discovered (McGale et al. 1996, Brickhouse and Dupree 1998), the color-activity and period-activity dependencies were studied on a bigger sample of 57 W UMa binaries (Stępień et al. 2001). But there is still no final theory describing the mechanism of X-ray emission.

Recently large databases of contact binaries were searched for coronal activity, offering still larger binary samples and thus better statistics. Geske et al. (2006) combined the Northern Sky Variability Survey (NSVS) catalogue with the ROSAT All-Sky Survey X-Ray catalogue and found 140 new binaries with active corona. A part of the All Sky Automated Survey (ASAS) catalogue (southern hemisphere) was also investigated (Chen et al. 2006), and 34 objects more were identified. In 2005 ASAS released the complete catalogue of variable stars south of declination +28deg (Pojmański et al. 2005), among which there are over 11,000 eclipsing binaries, thus providing the largest sample of galactic field binary stars.

In this short observational paper we combine the complete ASAS catalogue of variable stars (ACVS) with the ROSAT All-Sky Survey X-ray catalogue (RASS). We obtain the largest sample of X-ray active contact binary stars up to date, which constitutes 379 sources. Furthermore, we widen the study of stellar activity to include all types of eclipsing binaries i.e., including semi-detached and detached as well. The overall number of coincident sources amounts to 836. The overwhelming majority of the objects in our sample are close binaries that are expected to be in tidal synchronization. Therefore, we take the orbital period to be equal to the rotation period of each individual star.

Sections 2 and 3 describe both the ASAS and ROSAT catalogues, the process of preparing the combined sample and incidence of X-ray activity. In Section 4 we discuss the method of determining the bolometric and X-ray luminosities. The complete catalogue is presented in Section 5. A short analysis of the evolution of X-ray, or coronal, activity with rotation and colour is given in Section 6. We summarize the paper in Section 7.

## 2. The ASAS eclipsing binary catalogue

The All Sky Automated Survey (ASAS) is a blind optical survey that covers approximately 3/4 of the night sky. The scientific goal of ASAS is to study variability at the bright end ( $8 < V < 14$  mag), and at a moderate cadence (1-3 days). For the last 7 years, ASAS has been collecting data in both the  $V$ - and  $I$ - band. At this sampling rate and limiting magnitude, ASAS is optimized for studies of stellar variability. To date, ASAS has generated a rich  $V$ -band catalogue of over 50,000 classified variable stars.<sup>1</sup>

Roughly 20% (11,076) of the ASAS variable stars have been identified as eclipsing binaries (Pojmański 2002; Paczyński et al. 2006). The ASAS eclipsing binaries are divided into three classes, which are referred to as Eclipsing Contact (EC), Eclipsing Semi-Detached (ESD) and Eclipsing Detached (ED). Roughly 50% of the ASAS eclipsing binaries from the catalogue belong to the EC group while the other half is approximately evenly split between ESD and ED.

Note that the classification scheme of Pojmański (2002), that we employ here, differs from the more traditional convention of dividing eclipsing binaries into EW, EB and EA types. The (EC, ESD, ED) scheme discriminates between eclipsing binaries based upon the photometric smoothness of the eclipse. In the case of EC binaries, each eclipse is relatively smooth, while each eclipse is relatively sharp for the ED binaries. Therefore, the ratio of primary radius to orbital separation is relatively large for the EC systems while for ED binaries, this ratio is relatively small. A strong motivation for utilizing the Pojmański (2002) convention is the abundance of photometric data from ASAS as well as the (initial) lack of spectroscopic information for the ASAS variable star catalogue.

In this work, we take advantage of the  $I$ -band filter of ASAS, whose reduced photometric observations will soon be publicly available. As a result, we are able to utilize both photometric and color information of the 11,076 ASAS eclipsing binaries.

## 3. Combining the ASAS eclipsing binaries with ROSAT

The soft X-ray components of stellar spectra are primarily thought to originate from coronal activity. Stars on the main sequence that possess sizable outer convection zones exhibit increasing levels of coronal activity with increasing rotation rate. In particular, the ratio of X-ray to bolometric luminosity  $L_X/L_{\text{bol}}$  for G-F stars increases in proportion to the inverse of the Rossby number  $\text{Ro} = P/\tau_c$  squared (Schmitt et al. 1985), where  $P$  and  $\tau_c$  are the orbital period and convective turnover time of the primary, respectively. This relation holds as long as  $\text{Ro} \geq 1$ .

<sup>1</sup>Information on ASAS (Pojmański 1997, 1998, 2000, 2002, 2003, Pojmański and Maciejewski 2004, 2005, Pojmański, Pilecki and Szczygiel 2005) and its freely accessible data are located at <http://www.astrouw.edu.pl/asas>

The reduced data are available in both download-able ASCII format as well as an on-line database.

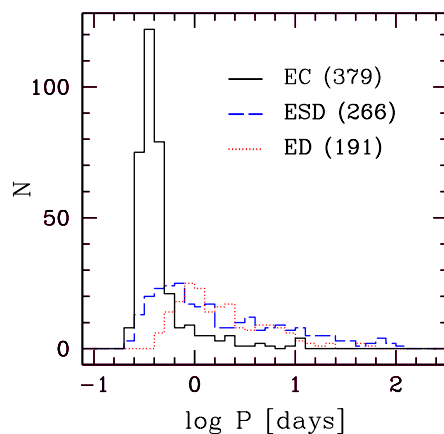


Fig. 1. Orbital period distribution of the ASAS eclipsing binaries that were matched with X-ray sources in the RASS catalogue.

As is readily shown in Fig. 1, an overwhelming majority of the ASAS eclipsing binaries possess orbital periods shorter than ten days (which is purely a result of observational selection) and hence, are tidally locked. It follows that most of the individual stars in Fig. 1 are rapidly rotating.

In order to study the relationship between coronal activity, rotation, and spectral type in the ASAS eclipsing binaries, a relatively deep wide-field X-ray survey is required. For these purposes, the best data set to date is given by the ROSAT All Sky Survey (RASS), which we briefly describe below.

### 3.1. Combined ROSAT and ASAS EB catalogue

Data for the RASS were taken primarily between 1990 and 1991 and holes in the survey were filled with pointed observations in 1997. The sky was scanned in  $2^\circ$  strips along the ecliptic and therefore regions of low ecliptic latitude were more thoroughly surveyed. The RASS covers between 0.1-2.4 keV in photon energy and entries are divided into a bright and faint source catalogue, consisting of 18,811 and 105,924 entries, respectively. Details on the ROSAT satellite and the RASS can be found in Voges et al. (1999).

We combine the ASAS eclipsing binary catalogue with the RASS Bright and Faint Source catalogues. The angular resolution of ASAS and RASS is  $\sim 15''/\text{pixel}$  and  $\sim 50''/\text{pixel}$ , respectively. The ROSAT angular resolution of  $\sim 50''$  determines whether or not a ROSAT source and a given ASAS eclipsing binary coincide with one another. In other words, as long as the angular separation between an ASAS eclipsing binary and an entry in RASS is less than  $50''$ , we assume that they are the same object. The distribution of angular separations for the coincident RASS and ASAS eclipsing binary sources are given in Fig. 2 (left panel).

The combination of both catalogues produces 836 matches. The majority of

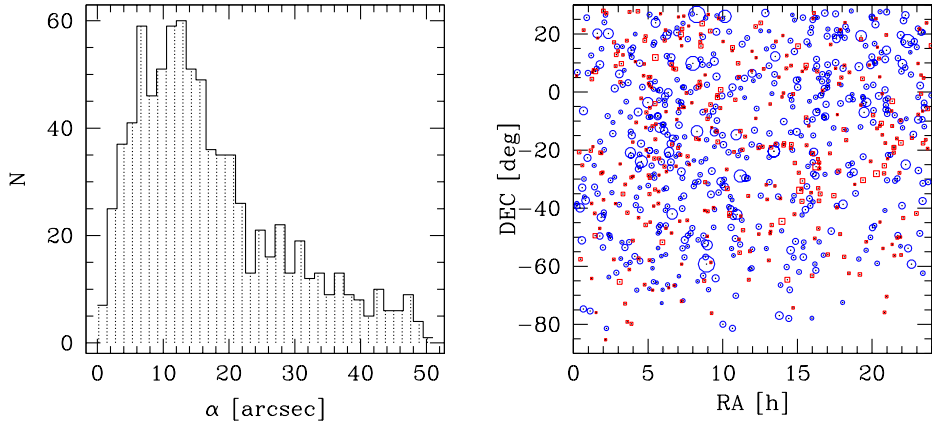


Fig. 2. Angular separation between matched pairs of the ASAS eclipsing binaries and the RASS X-ray sources is presented on the left panel. The right panel shows a distribution of objects in combined catalogues in equatorial coordinates. Blue circles correspond to ROSAT faint source catalogue, while red squares to ROSAT bright source catalogue. Symbol size corresponds to positional error in RASS catalogue.

matches (525) refer to the RASS faint source catalogue, while the remainder (311) to the bright source catalogue. The angular distribution of the ASAS-RASS coincident sources is plotted in the right panel of Fig. 2. For angular radius of  $50''$ , the possibility that our matches are polluted by background X-ray sources may draw concern.

We construct a false catalogue of eclipsing binaries by randomly shifting the right ascension and declination of each of the ASAS eclipsing binaries in between  $+5$  and  $-5$  degrees, similarly to the test performed by Geske et al. (2006). The resulting combination of the false eclipsing binary catalogue and RASS indicates the level of random coincidence. From this exercise, we find that only 1.4% of the matches between the real ASAS eclipsing binary catalogue and RASS are false at a separation of  $50''$ .

As a further check, we loosen the criteria for determining a match between the catalogues from an angular separation of  $50''$  up to  $90''$ . For the latter separation, we find that the number of matches between both catalogues increases to 942, where 615 and 327 belong to the faint and bright source catalogue, respectively. Thus, the increase in number of coincidences is largely due to sources belonging to the faint source catalogue. Though we increase the number of matches by  $\sim 10\%$  by relaxing our criteria for coincidence, the number of false matches increases to  $\sim 3.5\%$ . Nevertheless, from here on, we restrict our study to more conservative sample, which corresponds to a maximum angular separation of  $50''$  between RASS and ASAS eclipsing binary catalogues.

### 3.2. *Incidence of X-ray Activity*

The majority, if not all, of W UMa type variables are thought to be strong X-ray emitters. Cruddace and Dupree (1984) observed 17 W UMa stars, of which 14 showed X-ray activity. In the sample of Stępień et al. (2001) 57 out of 100 W UMa were X-ray sources (26 out of 31 closer than 100 pc). In the work of Geske et al. (2006) 140 X-ray sources were identified among 1022 galactic contact binaries, which constitutes 14%. However, when the sample is distance limited the percentage is higher - about 60% objects within 200 pc, 77% within 150 pc and 94% within 125 pc have detectable X-ray emission.

In our distance unlimited sample of 5,376 EC stars 379 exhibit X-ray activity, which constitutes 7%. We do not have distance estimates for objects which are not coronally active, so we cannot estimate the change of detection rate with distance. However, since the ASAS and NSVS projects are similar in the means of instrumentation and thus sky resolution and magnitude range, both detection rates should behave similarly with distance. We assume that roughly 80% of contact binaries closer than 150 pc display X-ray activity and in the following studies we will take a look both at the full sample of active binaries and at this closer subsample.

Since we did not limit our study to contact binaries only, we can estimate the incidence of X-ray activity among semi-detached and detached binaries. The former group contains 9% active sources (266 out of 2,957) and the latter 7% (191 out of 2,758). These values are close to the one for EC group, which suggests that there is a similar number of active binaries of each type.

## 4. Fluxes and Luminosities in the Optical and X-ray

As previously mentioned, there exists a relatively tight relationship between the stellar activity and the Rossby number for main sequence stars with convective envelopes. The resulting picture is that of magnetic dynamo processes converting convective and rotational energy into magnetic energy. Since magnetic structures are relatively buoyant in comparison to their surroundings, they have a tendency to rise to the surface, away from the region of their birth. The magnetic energy is dissipated high up in the atmosphere, above the photosphere, where the effective resistivity becomes large at relatively low densities. It is not clear how precisely this picture applies to close binary systems.

The combination of the ASAS eclipsing binary catalogue with RASS provides a sizable sample (836 sources) of binary stars that display some level of coronal activity. However, understanding of the relationship between the spectral type and rotation is less straightforward for binary systems than for single stars. Since a binary consists of two stellar components, it is not clear which of the individual components is responsible for the bulk of the stellar activity, though it is clear which component dominates the total stellar emission. For example, the V-band magnitude of any of the ASAS eclipsing binaries that we refer to is in reality, the

V-band magnitude at the maximum of the light curve. Therefore, the magnitude and color of the ASAS eclipsing binaries plotted in this paper are indicative of both components (but mostly of the primary), though either object may be dominant in X-rays.

For contact binaries the level of uncertainty is even greater. Neither of the components can truly be thought of as a main sequence stars from the perspective of a color-magnitude diagram. That is, a theoretical understanding of the relationship between surface temperature, effective gravity, and mass is not well understood for contact binaries.

#### 4.1. Bolometric Luminosity of Eclipsing Binaries

We parametrize the bolometric luminosity  $L_{\text{bol}}$  by the absolute magnitude in the V-band.

$$L_{\text{bol},\star} = L_{\text{bol},\odot} \times 10^{(M_{\text{bol},\odot} - M_{\text{bol},\star})/2.5} \quad (1)$$

$$M_{\text{bol},\star} = M_{V,\star} + BC \quad (2)$$

Absolute visual magnitudes ( $M_V$ ) are calculated from ( $V-I$ ) color; detached and semi detached systems were treated as single stars and for them we used a main sequence fit by Hawley et al. (1999), adopting solar metallicity. For contact binaries we applied a fit of Ruciński and Duerbeck (1997). With the help of *Hipparcos* parallax measurements, they derived a useful distance calibration for 40 nearby W UMa (contact) binaries. Since the authors claim, that the coefficients in the formula have large and non-Gaussian errors, we calculated distances to each star adopting two formulae - one utilizing V-band magnitude, and the other using I-band. We rejected 29 contact objects whose distance estimates differed by more than 20%.

Bolometric corrections ( $BC$ ) were calculated from a polynomial fit to the data given by Flower (1996), from the  $BC - T_{\text{eff}}$  relation, independent of luminosity classes. Effective temperatures were derived from the ( $V-I$ ) colour, based on calibration of Ramírez and Meléndez (2005).

We place the X-ray active ASAS eclipsing binaries on a color-magnitude diagram in Fig. 3. In this and following figures “EC best” (filled circles) denotes a subsample of the EC binaries, which are unambiguously classified as EC. Stars, whose type is uncertain are represented with open circles. Such objects are assigned multiple type in the process of the ASAS automated classification, e.g. EC/ESD or EC/BCEP/DSCT or EC/RRC (Pojmański, 2002). It happens usually when a light curve is of poor quality (eg. for faint stars), or when the amplitude is small (eg. low amplitude pulsating stars, single spotted rotating stars, etc.).

Note that all the EC binaries lie above the solid line representing the main sequence color-magnitude relation of Hawley et al. (1999) for local stars. Nevertheless, most of the EC sample lie close to the fit, with the majority lying about one magnitude above the main sequence relation. This is not unusual, since some of the

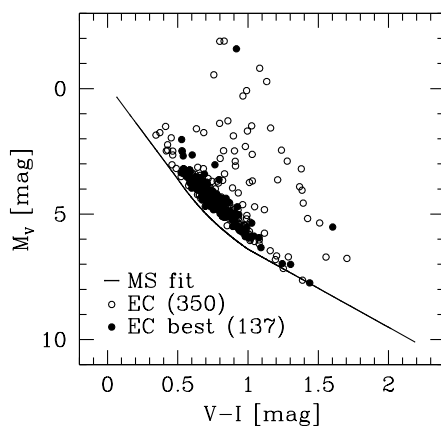


Fig. 3. The colour-magnitude diagram for EC, based on calibration of Ruciński and Duerbeck (1997). EC best is a subsample of all EC binaries, in which objects have a unique EC classification (see text). The line represents a MS relation for single stars derived by Hawley et al. (1999), which was adopted for ESD and ED variables.

contact binaries are the systems that have already evolved off the main sequence. Also, some scatter is probably due to mass ratio differences – similar spread is observed on a color-magnitude diagram for Hipparcos systems (Fig. 1 of Ruciński and Duerbeck 1997). The objects lying very far above the MS line might simply not be contact binaries (which is most probable in case of open circles), thus they do not obey an adequate color-magnitude relation.

For ESD and ED binaries in our sample, we assume that the luminosity of the system is dominated by the primary. Therefore we treat binaries which are either in marginal contact (ESDs) or detached (EDs) as single stars. This assumption may be dangerous when studying a relationship between X-ray emission and intrinsic physical parameters of the combined system e.g., the total bolometric luminosity, a size of the convection zone or orbital period. First, both stars may not be in close tidal contact and thus, the rotation period may differ from the orbital period. Furthermore, the primary star may not be a dominant source of the stellar activity.

The distance distribution for the three classes of eclipsing binaries that display coronal activity is displayed in Fig. 4. Systems that are in close contact (EC) are observed to further distances than semidetached and detached systems (ESD and ED), although most of the long tail among ECs is occupied by systems of multiple type (open circles in Fig. 3). Since ED are on average more luminous than EC and they are generally visible to further distances, this may suggest that EC have a higher level of X-ray activity than ESD and ED. On the other hand this may simply be a result of the selection effect - we observe twice as many EC than ED or ESD.

It is important to note that in the whole calculation process described in this section we did not account for interstellar extinction. This is justifiable in a close neighbourhood of the Sun, where we can assume that stars are unreddened, but be-



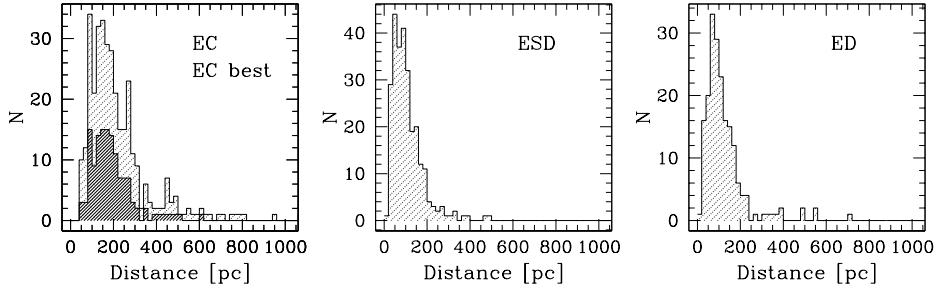


Fig. 4. Histograms of estimated distances of contact (EC), semi-detached (ESD) and detached (ED) eclipsing binaries. The most left image contains two histograms - the darker one is based on 'EC best' subsample.

comes a significant factor at larger distances and can introduce a high scatter when not taken into consideration. Due to this effect and the fact that the sample completeness deteriorates quickly with distance (as shown in Section 3.2), we choose a subsample of active binaries that lie within 150 pc from the Sun which consists of 127 EC, 214 ESD and 148 ED variables. In further study we will look both at the full sample and this distance limited subsample.

#### 4.2. X-ray Luminosity

The RASS data provide the number of photons per energy bin per unit time. The soft energy bin  $S$  corresponds to photons of energy 0.1-0.4 keV, while the hard bin  $H$  corresponds to photons with energies of 0.5-2.0 keV. Huensch et al. (1996) define a hardness ratio  $HR$

$$HR = \frac{H - S}{H + S}, \quad (3)$$

which is an important parameter in describing the X-ray spectral energy distribution. In terms of the hardness ratio, the X-ray flux  $f_X$  reads

$$f_X = CNTR \times (5.30HR + 8.7) \times 10^{-12} \text{ erg cm}^{-2} \text{ s}^{-1}. \quad (4)$$

where  $CNTR$  is the source count rate. The spectral energy distribution from which the above relation originates is based upon *ROSAT* observations of a complete, volume-limited sample of late-type giants (Huensch et al. 1996). This relation had been previously applied for W UMa type systems, whose X-ray emitting regions are believed to have similar properties as those of late-type giants (Chen et al. 2006, Stępień et al. 2001).

Finally, we calculate the X-ray luminosity

$$L_X = 4\pi d^2 f_X \quad (5)$$

of the eclipsing binary in question. The distance  $d$  was obtained from a distance modulus in the  $V$ -band.

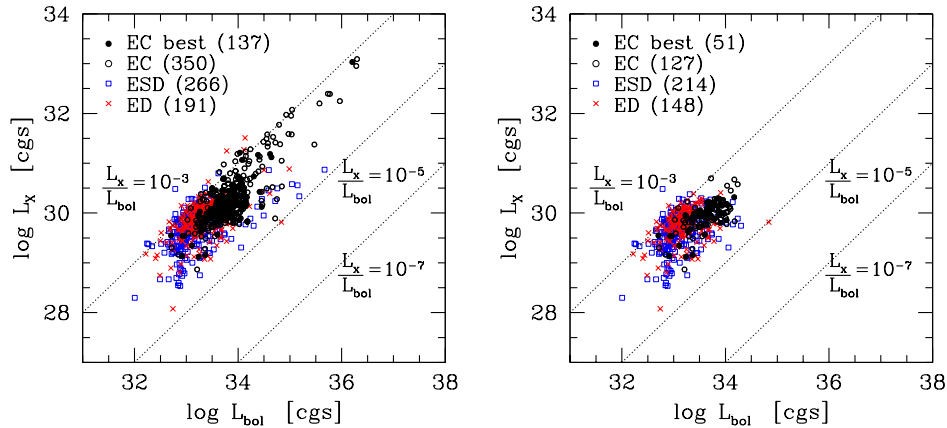


Fig. 5. Bolometric and X-ray luminosity function of 807 of the ASAS eclipsing binaries (left) and a distance limited subsample -  $d < 150pc$  (right). The overwhelming majority of these systems lie below  $L_X/L_{bol} = 10^{-3}$  (dotted line). EC binaries have higher  $L_{bol}$  than ESD and ED groups (this is better visible on a colour figure).

The X-ray vs. bolometric luminosity for the combined sample is given in Fig. 5. Almost all of the X-ray bright ASAS eclipsing binaries are active at a level between  $L_X/L_{bol} = 10^{-3}$  and  $L_X/L_{bol} = 10^{-4}$ . In this sample, and for our choice of bolometric calibration, EC binaries have higher  $L_{bol}$  than ESD and ED binaries, as was expected following Fig. 3.

## 5. The final catalogue

We produce a catalog of all ASAS eclipsing binaries for which we detected X-ray emission. All data are put in a single file "ASAS.ROSAT.cat" which contains 807 entries. The file is available for download from this website:

<http://www.astrouw.edu.pl/asas/?page=rosat>

Each line in the catalogue contains all basic information about a star, such as the ASAS and RASS IDs (ie coordinates), magnitudes, orbital period and all the information from the ACVS that might be useful for the catalogue users. Since the RASS catalogues are very large and are easily accessible, we only include a few quantities from RASS that were used in the course of this study, that is the hardness ratio and count rate and their errors. In addition, we supply the catalogue with the values that were calculated in the course of this study, such as distance,  $L_{bol}$ ,  $L_X$  and  $\log(Ro)$ . The detailed column descriptions as well as a few exemplary lines are presented in Table 1.

Table 1  
ASAS X-ray binaries catalogue.

ASAS ID	RASS ID	$\alpha$ [arcsec]	$P_{orb}$ [days]	$MJD_0$ [days]	V [mag]	I [mag]	d [pc]	$L_{bol}$ [erg/s]
030953-0653.6	J030952.6-065327	10.371	0.445286	1869.080	10.44	9.76	221.3182	34.006
203718-1047.5	J203718.3-104734	5.979	0.423600	1996.262	11.32	10.31	94.9199	33.037
233609-1628.2	J233608.7-162806	7.400	6.621000	1875.500	10.65	9.67	73.9801	33.076
.....								
.....	HR	HR err	CNTR [cts/s]	CNTR err [cts/s]	$L_X$ [erg/s]	$\log(P/\tau_c)$	Other ID	Type
[table continued]	1.00	0.78	0.059700	0.027530	30.690	-1.422	UX Eri	EC
	0.16	0.17	0.086610	0.016190	29.950	-	-	ESD
	1.00	0.29	0.064570	0.017100	29.772	-0.527	BQ Aqr	ED

A few exemplary lines of the ASAS catalogue of X-ray active binaries ASAS.ROSAT.cat. Each of the 807 lines contains star's ASAS ID and RASS ID, angular separation of both sources on the sky, orbital period of the binary,  $MJD_0$  ( $HJD_0 - 2450000$ ),  $V$  and  $I$  magnitudes at maximum light, distance  $d$ , bolometric luminosity  $L_{bol}$ , hardness ratio and its error, count rate and its error, X-ray luminosity  $L_X$  and a logarithm of Rossby number  $\log(P/\tau_c)$ . Last two columns contain other ID from the literature (mostly GCVS) and ACVS variability type (eg. EC, ESD, ED).

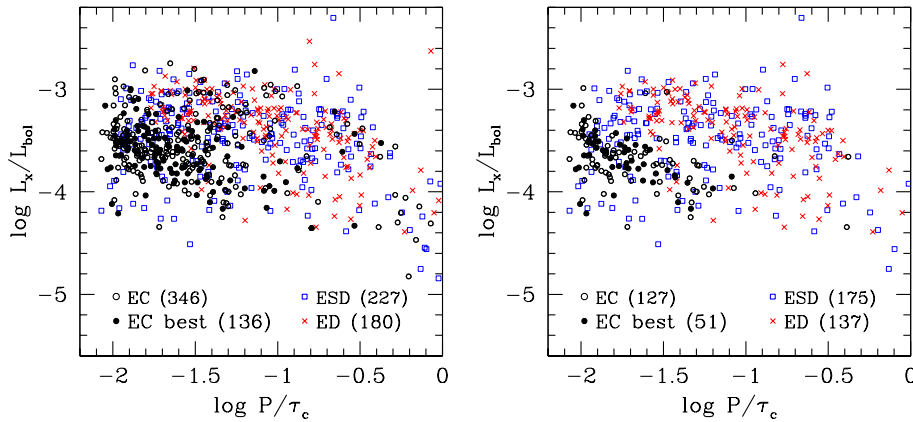


Fig. 6. The dependence of activity of the ASAS eclipsing binaries on the Rossby number, for objects with orbital periods less than 10 days (753). Left panel contains data points for all binaries and the right one for objects closer than 150 pc (439).

## 6. Relationship Between Coronal Activity, Rotation and Color

Binaries are more complicated than single stars, both on physical and observational grounds, particularly within the context of stellar activity. If indeed there is a physical connection between stellar activity, convection and rotation as is strongly suggested in the case of single dwarfs, then a similar trend may exist for binaries as well. Nevertheless, it seems difficult to easily disentangle – from both an observational and theoretical perspective – the salient physical parameters of a given binary for the purpose of quantifying its activity. Reasons for this difficulty have been previously mentioned.

In Fig. 6 the relationship between activity and the primary's Rossby number,  $Ro$ , is given for the coincident sources whose orbital periods are less than 10 days, which constitutes 753 objects. In order to calculate the Rossby number, the turnover time  $\tau_c$  for each star was extracted by the empirical formula provided by Stępień (2003). The turnover time is a function of  $(B-V)$  color, so we transform our  $(V-I)$  colors into  $(B-V)$  using the calibration of Caldwell et al. (1993). The fit of Stępień is valid for stars with  $(B-V) > 0.4$ , so for 34 objects which had this colour value lower, we adopt  $\log(\tau_c) = 0$ .

Note that relative to the turnover time, all of the binaries in Fig. 6 are rapid rotators. It follows that the binaries in our sample should be in the "saturated" state, in analogy with the observed phenomena in rapidly rotating single late-type dwarfs. That is, the coronal activity, quantified by  $L_X/L_{bol}$  should be constant with decreasing Rossby number  $Ro$ . The scatter of EC and ESD variables on the activity - Rossby number diagram is even larger than ECs, and we do not observe a clear increase of X-ray activity with decreasing rotational period for either group. We

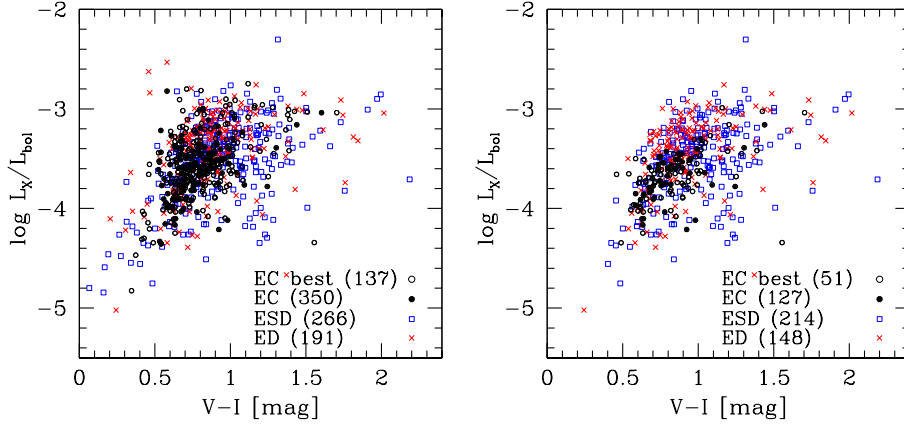


Fig. 7. Color-Activity diagram for the ASAS eclipsing binaries coincident with the RASS. Left panel contains data points for all 807 binaries and the right one for 489 objects closer than 150 pc.

note however, that ESDs and EDs are on average more active than ECs. To some degree, Fig. 6 displays the saturation effect in that the level of activity is roughly constant with decreasing Rossby number.

The same diagram for the limited sample ( $d < 150pc$ ) does not reduce the scatter in ESD and ED groups, but the trend of increasing activity with decreasing Ro is now clearly visible, especially among contact binaries.

There are claims (Stępień et al. 2001; Chen et al. 2006) that the so-called “super-saturation” phenomena – a reduction in coronal and chromospheric activity with *decreasing* Ro – is observed in extremely rapidly rotating isolated late type dwarfs *and* W UMa binaries. This subtle effect is not observed in Fig. 6, which is not surprising with the high scatter of points.

In Fig. 7, we plot an activity-color diagram for all the X-ray bright ASAS eclipsing binaries and for the subsample. Here, it is clear that the level of coronal activity indeed changes not only with the rotation, but surface temperature as well. With decreasing color index ( $V-I$ ), the surface temperature of the primary increases, while the depth of its convection zone decreases. So, binaries that are earlier type are less active in comparison to binaries that are later type. Of course, in this context “early” and “late” refer to surface temperature alone, rather than surface temperature and rotation as in the case of isolated stars.

Both Figs. 6 and 7 show that at a fixed overturn time and ( $V-I$ ) colour, the EC binaries are on average less active in comparison to ESD and ED systems. This is better visible on diagrams for the subsample of objects closer than 150 pc.

## 7. Summary

We had produced a catalogue of the combined ASAS eclipsing binaries and RASS X-ray sources. All data had been put in a single file "ASAS.ROSAT.cat" which is available for download from the ASAS website (<http://www.astrouw.edu.pl/asas/?page=rosat>) in the form presented in Table 1 (see Section 5 for details).

The combination of the eclipsing binary catalogue with the RASS produces a total of 836 coincident sources ( $\sim$  a 7% yield). Among these are 379 contact binary stars (EC), which is the largest sample of X-ray active contact binary stars assembled up to date. Semi-detached (ESD) and detached (ED) binaries were also taken into account, resulting in 266 and 191 active variables, respectively). We observe similar incidence of X-ray activity in all 3 groups of variables, which is around 7% in the distance unlimited sample.

An overwhelming majority of the coincident sources possesses orbital periods shorter than 10 days, so we expect tidal locking between the primary and the companion. Therefore, the orbital period of the binary may be also thought of as the rotation period of the stellar components.

We analyzed the dependence of X-ray activity on Rossby number and colour. In comparison to typical isolated stars of similar primary mass, the ASAS eclipsing binaries display a higher level of coronal activity (see Fig. 5) and the maximum value  $L_X/L_{\text{bol}} \sim 3 \times 10^{-3}$ , for the coincident sources is similar to that found in rapidly rotating isolated late-type dwarfs.

Both the activity - Rossby number (Fig. 6) and the activity - colour (Fig. 7) diagrams display a large scatter and they do not tighten any of the already known relations. The coronally-active binaries in our sample display the saturation effect, while there is no clear evidence of the so-called "super-saturation" effect.

However, for a given ( $V-I$ ) colour ECs are rotating more rapidly than the other two classes. And at the same time, for a given colour the level of activity of ECs is lower in comparison to ESDs and EDs. This slight downturn in activity among the three classes may in fact be an indirect manifestation of the saturation effect in Fig. 7.

**Acknowledgements.** We would like to thank K. Stępień for useful comments on the paper. This work was supported by the Polish MNiSW grants N203 007 31/1328 and N N203 304235. AS acknowledges support of a Hubble Fellowship administered by the Space Telescope Science Institute and of a Lyman Spitzer Jr. Fellowship at Astrophysical Sciences at Princeton University.

## REFERENCES

- Brickhouse, N. S., Dupree, A. K. 1998, *ApJ*, **502**, 918.  
 Caldwell, J. A. R., Cousins, A. W. J., Ahlers, C. C., van Wamelen, P., Maritz, E. J. 1993, *SAAOC*, **15**, 1.

- Carroll, R. W., Cruddace, R. G., Friedman, H., Byram, E. T., Wood, K., Meekins, J., Yentis, D., Share, G. H., Chubb, T. A. 1980, *ApJ*, **235**, 77.
- Chen, W. P., Sanchawala, Kaushar, Chiu, M. C. 2006, *AJ*, **131**, 990.
- Cruddace, R. G., Dupree, A. K. 1984, *ApJ*, **277**, 263.
- Duquennoy, A., Mayor, M. 1991, *A&A*, **248**, 485.
- Flower, P. J. 1996, *ApJ*, **469**, 355.
- Geske, M. T., Gettel, S. J., McKay, T. A. 2006, *AJ*, **131**, 633.
- Huensch, M., Schmitt, J. H. M. M., Schroeder, K.-P., Reimers, D. 1996, *A&A*, **310**, 801.
- Hawley, S. L., Tourtellot, J. G., Reid, I. N. 1999, *AJ*, **117**, 1341.
- McGale, P. A., Pye, J. P., Hodgkin, S. T. 1996, *MNRAS*, **280**, 627.
- Paczyński, B., Szczygieł, D. M., Pilecki, B., Pojmański, G. 2006, *MNRAS*, **368**, 1311.
- Pojmański, G. 1997, *AcA*, **47**, 467.
- Pojmański, G. 1998, *AcA*, **48**, 35.
- Pojmański, G. 2000, *AcA*, **50**, 177.
- Pojmański, G. 2002, *AcA*, **52**, 397.
- Pojmański, G. 2003, *AcA*, **53**, 341.
- Pojmański, G., and Maciejewski, G. 2004, *AcA*, **54**, 153.
- Pojmański, G., and Maciejewski, G. 2005, *AcA*, **55**, 97.
- Pojmański, G., Pilecki, B., Szczygieł, D. 2005, *AcA*, **55**, 275.
- Ramírez, I., Meléndez, J. 2005, *ApJ*, **626**, 465.
- Rucinski, S. M., Duerbeck, H. W. 1997, *PASP*, **109**, 1340.
- Schmitt, J. H. M. M., Golub, L., Harnden, F. R., Jr., Maxson, C. W., Rosner, R., Vaiana, G. S. 1985, *ApJ*, **290**, 307.
- Stępień, K., Schmitt, J. H. M. M., Voges, W. 2001, *A&A*, **370**, 157.
- Stępień, K. 2003, *IAU Symposium*, **210**, 716.
- Voges, W., et al. 1999, *A&A*, **349**, 389.